

06.5;05.3

Effect of annealing temperature on the kinetics of aluminum-induced crystallization of amorphous silicon suboxide thin films

© I.E. Merkulova^{1,2}, A.O. Zamchiy^{1,2}, N.A. Lunev¹, V.O. Konstantinov¹, E.A. Baranov¹

¹ Kutateladze Institute of Thermophysics, Siberian Branch, Russian Academy of Sciences, Novosibirsk, Russia

² Novosibirsk State University, Novosibirsk, Russia

E-mail: itpmerkulova@gmail.com

Received May 17, 2021

Revised July 20, 2021

Accepted July 21, 2021

In this work, the kinetics of aluminum-induced crystallization (AIC) of non-stoichiometric silicon oxide $a\text{-SiO}_{0.25}$ was investigated for the case of annealing at temperatures of 370, 385 and 400°C, as a result of which thin films of polycrystalline silicon were obtained. It is shown that, at low annealing temperatures, the surface morphology of the crystalline material is represented by dendritic structures corresponding to the growth model with diffusion-limited aggregation. In addition, with increasing annealing temperature, the nucleation density increases from 3 to 53 mm⁻². From the Arrhenius plot, the activation energy of the $a\text{-SiO}_{0.25}$ AIC was obtained for the first time and appeared to be 3.7 ± 0.4 eV.

Keywords: aluminum-induced crystallization, silicon suboxide thin films, polycrystalline silicon, activation energy.

DOI: 10.21883/TPL.2022.14.52059.18874

In recent times, an increase took place in the semiconductor industry demand for producing thin films of polycrystalline silicon (*poly*-Si) on low-cost low-temperature substrates, which are necessary for the photovoltaics and microelectronics [1,2]. One of the most common techniques for fabricating the *poly*-Si thin films is the metal-induced crystallization of amorphous silicon (*a*-Si) in which the process temperature and duration are reduced by using a metal (gold, nickel, aluminum). The aluminum-induced crystallization (AIC) of *a*-Si is an advanced method for the formation of high-quality thin film of *poly*-Si [3]. As known, the AIC of *a*-Si is defined by two stages, namely, nucleation and growth of the *poly*-Si crystals [4], therefore investigation of these stages provides deep understanding of the AIC process, which finally will enable the control and quality improvement of the obtained *poly*-Si films.

In addition, AIC of *a*-Si and properties of the obtained *poly*-Si films are strongly affected by impurities (e.g., oxygen) in the initial silicon-containing material. A few reports on AIC investigation for oxygen-containing films have been published [5,6] and showed that the problem of the oxygen influence needs more detailed study.

In this paper, analysis of kinetic processes was carried out, and the activation energy of the aluminum-induced crystallization of amorphous silicon suboxide ($a\text{-SiO}_x$, $0 < x < 2$) was obtained for the first time.

Using plasma enhanced chemical vapor deposition based on a wide-aperture source with inductive high-frequency excitation (13.56 MHz), thin $a\text{-SiO}_x$ films were synthesized from the $\text{SiH}_4\text{-O}_2$ gas mixture on the quartz and monocrystalline silicon substrates. The high-frequency radiation power was 50 W, while the substrate temperature was 150°C. Based on the IR transmission spectra measured with the Scimitar FTS 2000 setup, the initial film stoichiometric coefficient was determined ($x = 0.25$) [7]. As the

membrane layer, a native oxide layer obtained by exposing the samples to air was used [8]. After that, an aluminum layer was formed on the samples by the thermal vacuum evaporation. The $a\text{-SiO}_x$ film thickness (160 nm) and that of the Al film (130 nm) were acquired from images of the initial sample cross sections made with scanning electron microscope JEOL JSM-6700F. The obtained structures with the layer arrangement quartz/ $a\text{-SiO}_{0.25}$ / $a\text{-SiO}_2$ /Al were annealed in a vacuum furnace (10^{-5} Pa) at the temperatures of 370, 385 and 400°C for the time of up to 19 h. The vacuum furnace was equipped with optical microscope Navitar Zoom 6000 Ultrazoom for *in situ* observations.

Fig. 1 presents the optical-microscope images of samples annealed at 370, 385 and 400°C. As a result of layer exchange [9], nucleation and growth of the *poly*-Si crystalline structures were observed in the process of annealing on the side of aluminum [8]. Based on the optical-microscope images, it is possible to estimate the nucleation density that is one of the nucleation stage characteristics and directly depends on the annealing temperature. The nucleation density calculated for the samples under consideration increases with increasing annealing temperature and equals 3, 18 and 53 mm⁻² for temperatures of 370, 385 and 400°C, respectively. Based on the average *poly*-Si grain size obtained from the data presented in [9,10], the nucleation density was calculated for AIC of *a*-Si arranged as follows: substrate/Al/membrane layer/*a*-Si. Notice that the results obtained for the AIC of $a\text{-SiO}_x$ are about 100 times lower than the nucleation densities calculated for the AIC of *a*-Si. It is known that the decrease in the nucleation density leads to an increase in the average lateral size of the crystalline structure [11]. Thus, the low nucleation density obtained in this work confirms that the use of oxygen-containing films as silicon precursors promotes the

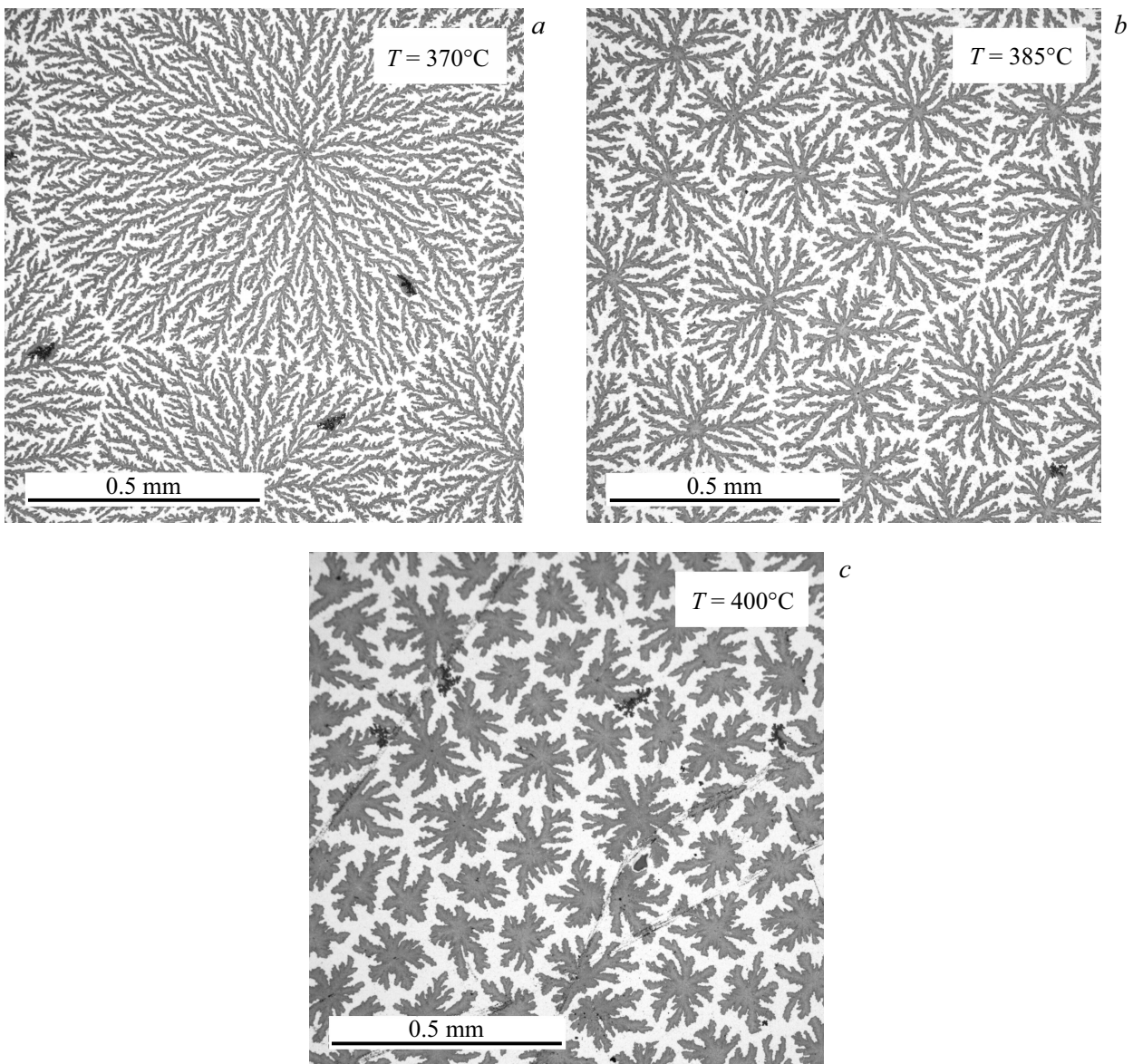


Figure 1. Optical microscope pictures of the sample surfaces annealed at 370 (a), 385 (b), 400°C (c).

increase in the average size of crystalline structures. At the low annealing temperatures (Figs. 1, a and b), the surface morphology has a form of fractal dendritic structures (dendrites) looking like a Brownian tree. This form conforms to the growth mathematical model described by the diffusion-limited aggregation (DLA) [12] since it is assumed that, with decreasing annealing temperature, the coefficient of Si atom diffusion into the Al layer becomes a key parameter affecting the crystalline structure growth rate. While the annealing temperature increases, the effect of the diffusion coefficient becomes weaker [13], which results in changes in the crystalline structure surface morphology (Fig. 1, c).

Notice that in annealing not only the silicon crystallization takes place but also an aluminothermal reaction causing the Si–O bond rupture and further oxidation of aluminum [6].

However, assessment of thermal effect of this reaction needs a separate analysis.

To describe the AIC of *a*-Si kinetics, the cover fraction (*CF*) curve is used, which represents the dependence of the sample covering with a crystalline material on the annealing time [14]. Using the surface images made during annealing with the optical microscope, *CF* values were obtained for the temperatures of 370, 385 and 400°C (Fig. 2). *CF* was calculated as a ratio between the crystalline structure area (dark regions in the image) and total area of the image. For all the temperatures, constant value *CF* = 54% was obtained, which means the completion of the AIC process. Such a value of *CF* results from the fact that the ratio between the initial film thicknesses *a*-SiO_x/Al in the sample was chosen lower than that necessary to form a continuous *poly*-Si film [15]. Notice that, when the temperature

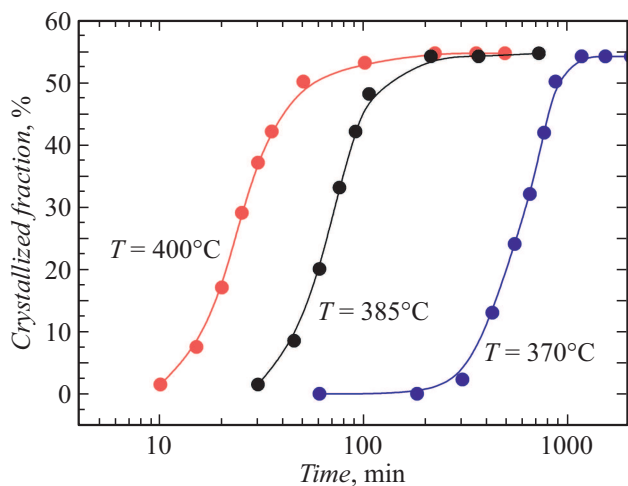


Figure 2. Cover fraction versus the annealing time for the annealing temperatures of 370, 385 and 400°C. The points are interpolated with lines for better visualization of the experimental results.

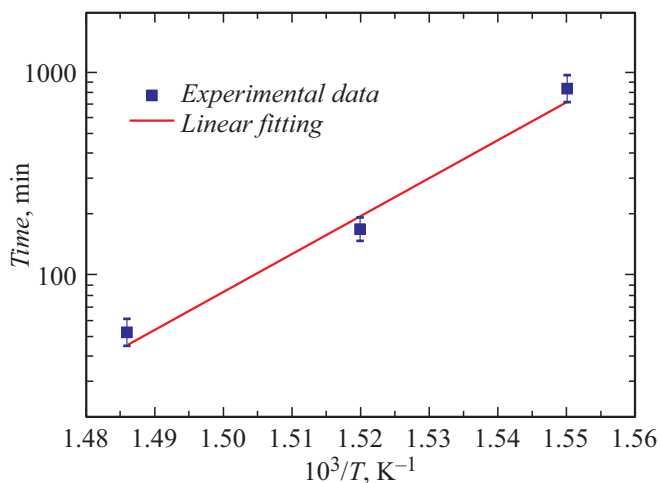


Figure 3. The Arrhenius plot for the annealing time corresponding to formation of the coating with $CF = 50\%$ versus the reciprocal annealing temperature.

increases from 370 to 400°C, the time necessary to reach $CF = 54\%$ decreases from 1020 to 180 min.

Fig. 3 presents the Arrhenius plot demonstrating the time necessary to form the film with $CF = 50\%$ versus the reciprocal temperature. The activation energy of the AIC of $a\text{-SiO}_{0.25}$ process was determined from the approximating straight line slope according to the procedure described in [16]; the energy appeared to be 3.7 ± 0.4 eV. The obtained value is higher than the AIC of $a\text{-Si}$ activation energies ranging from 1.04 [17] to 1.9 eV [4].

Thus, in this work kinetics of the aluminum-induced crystallization of non-stoichiometric silicon oxide $a\text{-SiO}_{0.25}$ was studied at annealing temperatures of 370, 385 and 400°C. The nucleation density increases with increasing temperature from 3 to 53 mm^{-2} that is essentially lower than for the AIC of $a\text{-Si}$. The paper has shown that

at low annealing temperature the surface morphology is represented by dendritic structures corresponding to the DLA growth model. Using the Arrhenius plot, the AIC of $a\text{-SiO}_{0.25}$ activation energy was obtained for the first time; it was 3.7 ± 0.4 eV.

Financial support

The study was financially supported by the Russian Scientific Foundation (project № 19-79-10143).

Conflict of interests

The authors declare that they have no conflict of interests.

References

- [1] G. Maity, R. Singhal, S. Dubey, S. Ojha, P.K. Kulriya, S. Dhar, T. Som, D. Kanjilal, S.P. Patel, *J. Non-Cryst. Solids*, **523**, 119628 (2019). DOI: 10.1016/j.jnoncrysol.2019.119628
- [2] T. Nguyen, M. Hiraiwa, T. Koganezawa, S. Yasuno, S.-I. Kuroki, *Jpn. J. Appl. Phys.*, **57**, 031302 (2018). DOI: 10.7567/JJAP.57.031302
- [3] K. Toko, T. Suemasu, *J. Phys. D: Appl. Phys.*, **53**, 373002 (2020). DOI: 10.1088/1361-6463/ab91ec
- [4] J. Schneider, J. Klein, M. Muske, S. Gall, W. Fuhs, *J. Non-Cryst. Solids*, **338**, 127 (2004). DOI: 10.1016/j.jnoncrysol.2004.02.036
- [5] J.H. Yoon, *Phys. Status Solidi RRL*, **10**, 668 (2016). DOI: 10.1002/pssr.201600198
- [6] A.O. Zamchiy, E.A. Baranov, I.E. Merkulova, I.V. Korolkov, V.I. Vdovin, A.K. Gutakovskii, V.A. Volodin, *Mater. Lett.*, **293**, 129723 (2021). DOI: 10.1016/j.matlet.2021.129723
- [7] A.O. Zamchiy, E.A. Baranov, I.E. Merkulova, S.Ya. Khmel, E.A. Maximovskiy, *J. Non-Cryst. Solids*, **518**, 43 (2019). DOI: 10.1016/j.jnoncrysol.2019.05.015
- [8] A.O. Zamchiy, E.A. Baranov, E.A. Maximovskiy, V.A. Volodin, V.I. Vdovin, A.K. Gutakovskii, I.V. Korolkov, *Mater. Lett.*, **261**, 127086 (2020). DOI: 10.1016/j.matlet.2019.127086
- [9] W. Duan, F. Meng, J. Bian, J. Yu, L. Zhang, Z. Liu, *Appl. Surf. Sci.*, **327**, 37 (2015). DOI: 10.1016/j.apsusc.2014.11.098
- [10] R. Numata, T. Kaoru, U. Noritaka, S. Takashi, *Thin Solid Films*, **557**, 147 (2014). DOI: 10.1016/j.tsf.2013.08.044
- [11] J. Chen, J. Suwardy, T. Subramani, W. Jevasuwan, T. Takei, K. Toko, T. Suemasu, N. Fukata, *CrystEngComm*, **19**, 2305 (2017). DOI: 10.1039/C6CE02328B
- [12] T.A. Witten, Jr., L.M. Sander, *Phys. Rev. Lett.*, **47**, 1400 (1981). DOI: 10.1103/PhysRevLett.47.1400
- [13] L.M. Sander, *Contemp. Phys.*, **41**, 203 (2000). DOI: 10.1080/001075100409698
- [14] S. Gall, M. Muske, I. Sieber, O. Nast, W. Fuhs, *J. Non-Cryst. Solids*, **299**, 741 (2002). DOI: 10.1016/S0022-3093(01)01108-5
- [15] A.O. Zamchiy, E.A. Baranov, S.Ya. Khmel, V.A. Volodin, V.I. Vdovin, A.K. Gutakovskii, *Appl. Phys. A*, **124**, 646 (2018). DOI: 10.1007/s00339-018-2070-y
- [16] C.J. Meechan, J.A. Brinkman, *Phys. Rev.*, **103**, 1193 (1956). DOI: 10.1103/PhysRev.103.1193
- [17] P.I. Widenborg, A.G. Aberle, *J. Cryst. Growth*, **242**, 270 (2002). DOI: 10.1016/S0022-0248(02)01388-X